# The Vinyl + NO Reaction: Determining the Products with Time-Resolved Fourier Transform Spectroscopy

**Peng Zou, Stephen J. Klippenstein, and David L. Osborn***

*Combustion Research Facility, Sandia National Laboratories, P.O. Box 969, Livermore, California 94551-0969*

*Received: January 6, 2005; In Final Form: April 12, 2005*

We have studied the vinyl + NO reaction using time-resolved Fourier transform emission spectroscopy, complemented by electronic structure and microcanonical RRKM rate coefficient calculations. To unambiguously determine the reaction products, three precursors are used to produce the vinyl radical by laser photolysis: vinyl bromide, methyl vinyl ketone, and vinyl iodide. The emission spectra and theoretical calculations indicate that HCN + $CH_2O$ is the only significant product channel for the $C_2H_3$ + NO reaction near room temperature, in contradiction to several reports in the literature. Although CO emission is observed when vinyl bromide is used as the precursor, it arises from the reaction of NO with photofragments other than vinyl. This conclusion is supported by the absence of CO emission when vinyl iodide or methyl vinyl ketone is used. Prompt emission from vibrationally excited NO is evidence of the competition between back dissociation and isomerization of the initially formed nitrosoethylene adduct, consistent with previous work on the pressure dependence of this reaction. Our calculations indicate that production of products is dominated by the low energy portion of the energy distribution. The calculation also predicts an upper bound of 0.19% for the branching ratio of the $H_2CNH$ + CO channel, which is consistent with our experimental results.

## I. Introduction

The chemistry of unsaturated hydrocarbon free radicals has been the focus of numerous studies because of its importance in combustion as well as interstellar chemical reactions.[1] The vinyl radical ($C_2H_3$) is among the simplest unsaturated hydrocarbon free radicals and is an important intermediate in the combustion of aliphatic fuels. The vinyl radical can be found in the combustion processes of most aliphatic fuels and its reactions will, therefore, influence chemical pathways and final product distributions. The vinyl radical may contribute to the formation of polycyclic aromatic hydrocarbons (PAH) and growth of soot depending on pressure, temperature, and composition of fuel mixture.[2] Furthermore, a detailed understanding of the vinyl radical reaction with NO is important to understanding the fuel reburning[3,4] processes that reduce $NO_x$ emissions in combustion.

There are a number of studies on the $C_2H_3$ + NO reaction[5−12] and many of these experiments focus on the inhibition role of NO in the pyrolysis of acetylene and are usually performed in $C_2H_2$/NO mixtures. There are several reaction pathways of $C_2H_3$ + NO that are thermodynamically accessible at room temperature (eqs 1a−f).

$$C_2H_3 + NO \rightarrow C_2H_3NO \qquad \Delta_rH^\circ_{298K} = -52.0 \text{ kcal/mol} \quad (1a)$$

$$\rightarrow HCN + CH_2O \qquad \Delta_rH^\circ_{298K} = -88.0 \text{ kcal/mol} \quad (1b)$$

$$\rightarrow H_2CNH + CO \qquad \Delta_rH^\circ_{298K} = -93.0 \text{ kcal/mol}^{13} \quad (1c)$$

$$\rightarrow NCO + CH_3 \qquad \Delta_rH^\circ_{298K} = -27.4 \text{ kcal/mol} \quad (1d)$$

$$\rightarrow H_2CCN + OH \qquad \Delta_rH^\circ_{298K} = -24.7 \text{ kcal/mol} \quad (1e)$$

$$\rightarrow HNCO + CH_2 \qquad \Delta_rH^\circ_{298K} = -24.5 \text{ kcal/mol} \quad (1f)$$

A schematic diagram of the potential energy surface (PES) of channels 1a−c is shown in Figure 1.

Sherwood and Gunning[5,6] observed that HCN and $CH_2O$ are the dominant products of the title reaction at pressures from 2 to 40 Torr at room temperature. In their experiments, the vinyl radical was produced by the recombination reaction H + $C_2H_2$, with H atoms produced by either $H_2S$ photolysis[5] or mercury-photosensitized decomposition of acetylene.[6] The end products were analyzed by gas chromatography and mass spectrometry. The authors suggested that the reaction proceeds through an OCCN four-membered-ring intermediate (1,2-oxazete) followed by N−O and C−C bond breaking and applied this mechanism to explain the results of other substituted vinyl radicals and NO reactions they studied. This reaction mechanism is supported by the model analysis of Benson,[7] which is based primarily on the shock tube data of Ogura[8] on the pyrolysis of $C_2H_2$/NO mixtures. Besides the primary products, Sherwood and Gunning also observed small amounts of CO (<13%), but did not postulate its sources. In a more recent experimental study, Feng et al.[12] assigned signal in the $C_2H_3$ + NO reaction to products from channels 1b−e using low resolution (16 $cm^{-1}$), time-resolved Fourier transform emission spectroscopy (TR-FTS).

The only measurement of the rate coefficient of $C_2H_3$ + NO is due to Striebel et al.,[11] who used the pulsed laser photolysis/

* Corresponding author. E-mail: dlosbor@sandia.gov.

10.1021/jp050093c CCC: $30.25 
Published on Web 05/14/2005

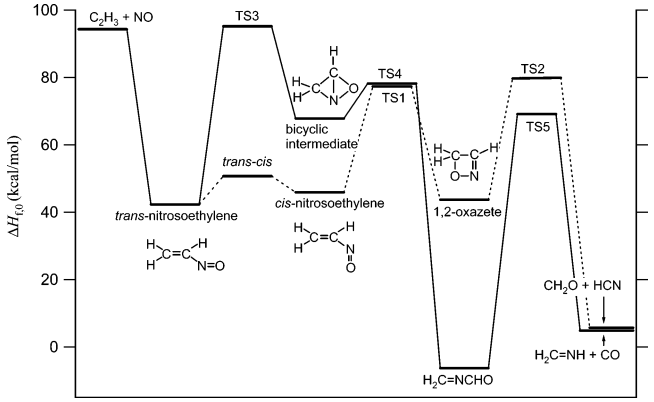


**Figure 1.** Schematic energy diagram of the $C_2H_3$ + NO reaction. The dotted and solid lines represent pathways to $CH_2O$ + HCN (eq 1b) and $H_2CNH$ + CO (eq 1c), respectively. The stationary point energies are from ref 11 except for $H_2CNH$ + CO and TS5, which are from this work. All the energies are calculated at the QCISD(T) level extrapolated to the infinite basis set limit and corrected with zero-point energy evaluated at the B3LYP/6-311++G(d,p) level.

cw laser absorption technique to monitor the disappearance of $C_2H_3$. They measured the room-temperature removal rate coefficient of vinyl radical by NO to be $1.6 \pm 0.4 \times 10^{-11}$ cm$^3$ molecule$^{-1}$ s$^{-1}$ with only modest pressure dependence from 10 to 160 Torr of helium. Fall off of the rate coefficient to lower pressure was observed at higher temperature, 400−700 K. The reaction rate coefficient was also found to have a strong negative temperature dependence.

There are three electronic structure investigations of the potential energy surface for the $C_2H_3$ + NO reaction.[9−11] Arulmozhiraja and Kolandaivel performed ab initio calculations to investigate the stability and geometries of several isomers of $C_2H_3NO$ at both Hartree−Fock and second-order Møller−Plesset (MP2) levels of theory with basis sets up to 6-311G*.[9] Sumathi et al.[10] performed higher level ab initio calculations, employing both MP2 and CCSD(T) with the 6-311++G(d,p) basis set. They suggest that the HCN + $CH_2O$ channel is dominant at high temperature, but the $C_2H_3$ + NO reaction cannot proceed beyond the oxazete intermediate at room temperature due to a high barrier for dissociation of the oxazete intermediate. This conclusion contradicts the observations of Sherwood and Gunning,[6] Benson,[7] and Ogura.[8] More recent calculations of Striebel et al. at the QCISD(T) level, and, as necessary, the multireference configuration interaction (MRCI) level, indicate that the formation and dissociation of the oxazete ring proceeds via tight transition states, in agreement with Sumathi et al.[10] However, these transition states (TS1 and TS2 in Figure 1) are predicted to lie ∼15 kcal/mol below the $C_2H_3$ + NO asymptote, substantially lower than in the previous results of Sumathi et al. Using their ab initio potential energy surface with these lower barrier heights, Striebel et al. satisfactorily reproduced the measured temperature and pressure dependence of the rate coefficient with an RRKM theory-based master equation calculation. This calculated rate coefficient drops too slowly with decreasing pressure to be consistent with termination of the reaction at the 1,2-oxazete intermediate, as suggested by Sumathi et al. In addition, Striebel et al. found a much lower energy pathway to $H_2CNCHO$ through a bicyclic intermediate, shown as the solid line path in Figure 1, which could produce $H_2CNH$ and CO by H-migration and N−C bond fission.

In this paper, we present experimental and theoretical results to resolve the discrepancy in the literature on the product identities and reaction mechanism of the vinyl + NO reaction. Even with a time-resolved technique, the effects of reactions involving species arising from all photolysis channels of the vinyl precursor must be carefully considered. The disparate experimental and theoretical results in the literature, together with the newly found lower energy pathway of channel 1c, motivated us to examine the emission from products at a resolution high enough to accurately assign rotationally resolved emission bands using TR-FTS. Furthermore, the vinyl radical is produced by photolysis of three different precursors: vinyl bromide (VB), methyl vinyl ketone (MVK), and vinyl iodide (VI). By using different precursors, we are able to distinguish the products from secondary or competing chemistry introduced into the system by photolysis, which allows us to unambiguously assign the products of the title reaction.

## II. Experimental Section

The TR-FTS apparatus used in the present experiment has been described in detail previously.[14,15] Sample gases are delivered into a Teflon-lined stainless steel flow cell through calibrated mass flow controllers. Vinyl radicals are produced by the photolysis of VB or MVK at 193 nm or of VI at 248 nm. Typical laser pulse width is ∼20 ns at a 30 Hz repetition rate with a fluence of 20−30 mJ cm$^{-2}$ pulse$^{-1}$ at 193 nm and 40−60 mJ cm$^{-2}$ pulse$^{-1}$ at 248 nm. Time-resolved emission from vibrationally excited reactants and products is collected perpendicular to the photolysis beam by Welsh collection optics[16] made from a pair of 10 cm diameter gold or silver-coated spherical mirrors. The transient signal is sent into an evacuated Fourier transform spectrometer (Bruker IFS 66v/S) operating in step-scan mode[17] and detected by either a liquid nitrogen cooled indium antimonide (InSb) or mercury cadmium telluride (MCT) photodiode detector. The signal is amplified and digitized by a 16-bit 200 kS/s digitizer. The spectra are generally taken with 0.5 cm$^{-1}$ spectral and 5 $\mu$s temporal resolution.

Because the vinyl radical produced by photolysis possesses significant internal energy, either helium or argon is used as a buffer gas to study the effects of vibrational relaxation of vinyl on the reaction product formation. The pressure of the cell is measured by a capacitance manometer and maintained at 1−2 Torr through a closed-loop feedback valve throttling the pump with <1% variation during the experiments. Experiments are also performed with pressure up to 8 Torr to study the effect of relaxation with either He or Ar buffer gases. The mixing ratios of the precursors are generally <3% and that of NO is ∼5−10% in the cell. The absorption cross sections[18,19] (in cm$^2$ molecule$^{-1}$, base e) of the three precursors are the following: VB(193 nm) = $3.1 \times 10^{-17}$, MVK(193 nm) = $3.2 \times 10^{-17}$, and VI(248 nm) = $9.9 \pm 0.3 \times 10^{-19}$ (measured in this work). The resulting number density of $C_2H_3$ radicals produced by laser photolysis is estimated to be $10^{13}$−$10^{14}$ molecule cm$^{-3}$, which is ∼10−70 times less than the NO concentration, ensuring pseudo-first-order reaction conditions and minimizing secondary reactions of the vinyl radical. Using VB as the vinyl precursor produces the strongest total signal, but also leads to complications that are resolved by use of MVK and VI precursors. We considered other vinyl precursors, but found them inadequate. Vinyl chloride photodissociation at 193 nm produces HCl, $H_2$, and H as primary dissociation channels.[20] UV photolysis of 1,3-butadiene also involves multiple product channels, and the yield of $C_2H_3$ + $C_2H_3$ is only 8% at 193 nm.[21]

Helium (99.999% Matheson) and argon (99.999% Matheson) gases are used without further purification. Vinyl bromide (98%), vinyl iodide (98%), and methyl vinyl ketone (99%) are obtained from commercial sources and used after several

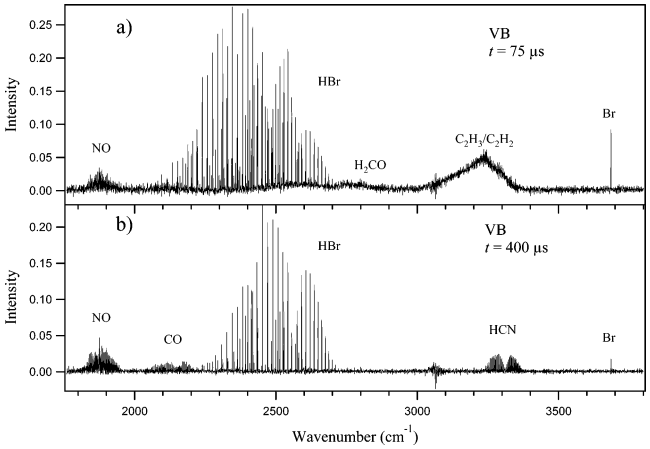


**Figure 2.** Representative emission spectra at a resolution of 0.5 $cm^{-1}$ of the $C_2H_3$ + NO reaction taken at (a) $t = 75$ $\mu$s and (b) $t = 400$ $\mu$s time delays, respectively, using VB as the vinyl precursor.

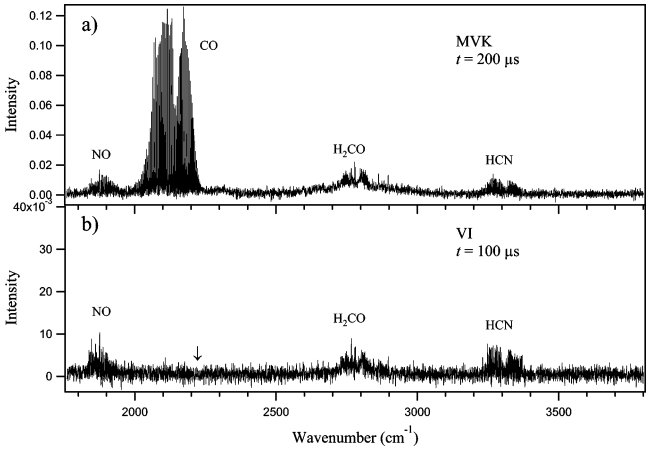


**Figure 3.** Representative emission spectra at a resolution of 0.5 $cm^{-1}$ of the $C_2H_3$ + NO reaction, using MVK (a) and VI (b) as precursors of vinyl. The arrow indicates the center of the (unobserved) HI emission band at 2230 $cm^{-1}$.

freeze−pump−thaw degassing cycles. NO (99.0% Matheson) is flowed through a molecular sieve purifier prior to being delivered into the cell to remove the major impurities $N_2O$ and $CO_2$. The purity of the NO is checked with FTIR absorption spectroscopy.

## III. Results and Analysis

**A. Assignment of Emission Bands.** In this experiment, time-resolved infrared emission may arise from hot photolysis fragments, products of the title reaction, products of competing or secondary reactions, and molecules excited by energy transfer. Representative emission spectra at short (75 $\mu$s) and long (400 $\mu$s) time delays are shown in Figure 2, taken with VB as the vinyl precursor and an InSb detector. Spectra collected with MVK and VI as vinyl precursors are shown in Figure 3, parts a and b, taken at $t = 200$ and 100 $\mu$s, respectively. The emission intensity from each species is fit by using a nonlinear least-squares fitting procedure that has been described in detail previously.[15,22] Rovibrational line positions are calculated from the spectroscopic constants for CO,[23] HBr,[24] NO,[25] HCCH,[26] HCN,[27] and $CH_2O$.[28,29] Representative fitting results, shown in Figure 4, demonstrate that we can unambiguously identify these molecules. During the fitting of NO spectra, we correct for the "cold gas filter" effect due to absorption of 1→0 emission by the high concentration of $v = 0$ NO.

When VB is used as the precursor, we observe HBr and Br, arising from molecular elimination and direct C−Br bond fission of VB, respectively. The sharp emission line at 3685.2 $cm^{-1}$ in Figure 2 is the transition of spin−orbit excited Br ($^2P_{1/2}$) to its ground state ($^2P_{3/2}$).[30] The HBr emission, from 2000 to 2800 $cm^{-1}$, has high signal intensity and is easily rotationally resolved. Because rotational relaxation occurs on the time scale of several collisions for all species, the rotational temperature derived from fitting of HBr spectra can be used as a fixed rotational temperature during fitting of other species. Fitting the HBr spectra at different time delays confirms rapid rotational equilibration, resulting in the same rotational temperature at all delays, which on average is 350 ± 50 K for all HBr vibrational bands. This rotational temperature agrees very well with the results from the fitting of other linear molecules observed in these experiments. Therefore, we fix the rotational temperature at 350 K during the fitting of spectra in which a rotational temperature is not easily derived due to spectral congestion or a low signal-to-noise ratio.

Because vibrational relaxation of HBr is enhanced by the introduction of NO, it is not viable to remove the emission of HBr by simple subtraction of time-resolved emission with and without NO present. In contrast to the vinyl bromide precursor, we observe no HI emission at 2230 $cm^{-1}$ when VI is photodissociated (Figure 3b), implying that the only significant dissociation channel for VI at 248 nm is $C_2H_3 + I(^2P_J)$.

We observe $CH_2O$ emission for all the precursors used as shown in Figures 2a and 3. The $CH_2O$ emission, centered at ~2760 $cm^{-1}$, is comprised of both $\Delta v_5 = -1$ (*b*-type $CH_2$ asymmetric stretch mode) and $\Delta v_1 = -1$ (*a*-type $CH_2$ symmetric stretch mode) bands. The $CH_2O$ emission is absent at $t = 400$ $\mu$s in Figure 2b because the relaxation of $CH_2O$ is faster than that of other vibrationally excited species (NO, HCN, CO, HBr), and cannot be observed at long time delay, especially when VB is the precursor. One time slice of $CH_2O$ (with VI as the vinyl precursor) is shown in Figure 4. The time-resolved spectra are fit assuming Boltzmann rotational and vibrational distributions with a common vibrational temperature for both $\nu_5$ and $\nu_1$ bands. The rotational temperature is fixed at 350 K, as discussed previously, while the vibrational temperature and total intensity are varied to give the best fit. The asymmetric reduced form of the Watson Hamiltonian[31] and previously measured spectroscopic constants[28,29] provide the line positions. The contribution of $\Delta v_5 = -1$ and $\Delta v_1 = -1$ bands are weighted by their Einstein *A* coefficients ($A_{1\rightarrow0} = 73.2$ and 88.6 $s^{-1}$ for the $\nu_1$ and $\nu_5$ modes, respectively).[32] We assume the harmonic oscillator dependence of the *A* coefficients on vibrational quantum number, i.e., $A_{n\rightarrow m} = nA_{1\rightarrow0}$. For the sake of simplicity and also due to the moderate experimental resolution, we ignore vibration−rotation interaction and assume the rotational profiles of all bands are identical with their fundamental bands, only being shifted according to the vibrational anharmonicity parameters measured with dispersed fluorescence spectroscopy.[29] Both $\nu_1$ and $\nu_5$ bands must be included to obtain a satisfactory fit. The reasonable fit shown in Figure 4 indicates that, although greatly simplified, the model used here clearly identifies $CH_2O$ and provides important information on its vibrational distribution. We also attempted to measure the C═O stretching band of $CH_2O$ at 1746 $cm^{-1}$ using the MCT detector, but did not observe any obvious emission due to the lower sensitivity of the detector and a smaller Einstein *A* coefficient of 28 $s^{-1}$.[32]

In the C−H stretching region, the broad emission centered at ~3250 $cm^{-1}$ in Figure 2a is primarily $\Delta v_3 = -1$ bands of

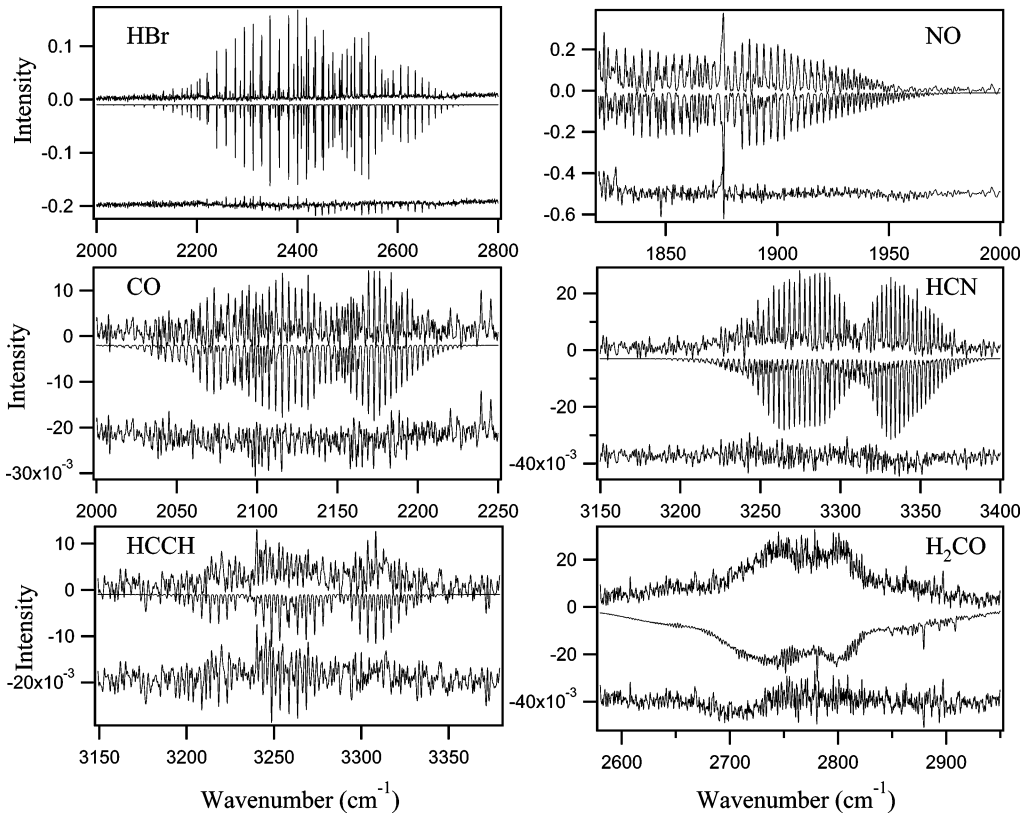


**Figure 4.** Emission spectra (upper trace in each panel) of different species with corresponding fits and residuals. Fits are inverted and displaced; residuals are displaced for clarity.

acetylene,[26] which is the counter photofragment of HBr from the photodissociation of VB. The $\nu_1$, $\nu_2$, and $\nu_3$ C−H stretching bands of the vinyl radical[33] could also contribute in this region. According to Wodtke et al.,[34] the branching ratio $[C_2H_3]/[C_2H_2] = 0.56/0.44$ in dissociation of VB at 193 nm. At the B3LYP/cc-pVTZ level, the calculated Einstein *A* coefficients for the three vinyl bands are 0.8, 4.7, and 6.1 $s^{-1}$, respectively, while the experimental *A* coefficient for the $\nu_3$ band of acetylene is 36 $s^{-1}$. Therefore acetylene, not vinyl, should be the major contributor to the broad emission at ~3250 $cm^{-1}$ in Figure 2a. Given sufficient time for partial vibrational relaxation, the $\Delta v_3 = -1$ bands of HCCH can be rotationally resolved in vinyl bromide photodissociation without NO present, as shown in Figure 4. HCCH emission is not seen at long delay times when NO is present because the introduction of NO significantly increases the relaxation rate of vibrationally excited HCCH.[35] As the final contribution to this region, the $\nu_1$ band of HCN can be partially distinguished on top of the broad emission in Figure 2a, and is clearly seen in Figures 2b and 3. Since the noise level in TR-FTS is proportional to the incident light intensity on the detector, the spectra at short time delay are generally noisier than spectra at longer time delay. Therefore, rotationally resolved emission bands from HCN are more easily observed at longer delay times, when the baseline becomes less noisy and emission from other vibrationally excited molecules is removed by either collisional relaxation or reaction with NO.

When VI is used as the precursor with [NO] = 0, emission in the C−H stretch region can only arise from the $C_2H_3$ radical. By comparing the temporal profile of integrated emission intensity in the C−H stretch region taken with and without NO, we find that the relaxation of vinyl radical by NO occurs in less than 5 $\mu$s (the temporal resolution of the current experiments). The data provide a lower limit on the vibrational relaxation rate coefficient of vinyl by NO of $k_{relax} \geq 3 \times 10^{-11}$ $cm^3$ $molecule^{-1}$ $s^{-1}$.

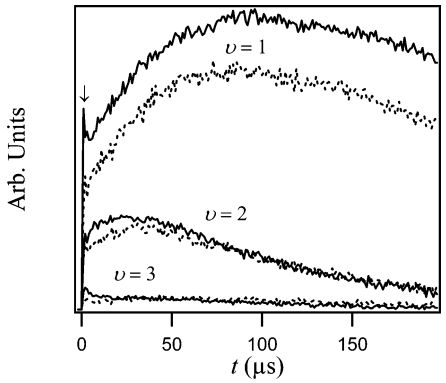


**Figure 5.** Temporal profiles of different vibrational states of NO. Solid and dotted lines represent $^2\Pi_{1/2}$ and $^2\Pi_{3/2}$ states, respectively. Data points from the earliest time slices have larger uncertainty than at later time due to the higher noise level at short time delays. The spike in the $v = 1$ population (indicated by the arrow immediately after the laser flash) results from a fitting artifact caused by these higher noise levels.

The emission centered at 1876 $cm^{-1}$ is assigned to $\Delta v = -1$ bands of NO $X(^2\Pi)$ and can be seen in both Figures 2 and 3 using different precursors. We verified that the infrared emission from NO does not result from electronic excitation of NO by the photolysis laser, followed by E → V energy transfer, by running experiments with the vinyl precursor replaced by helium: no emission is observed under these conditions. The temporal profiles of $v = 1-3$ populations in both spin−orbit states are shown in Figure 5, using VB as precursor of vinyl. Significant amounts of $v = 1$, 2 and very little $v = 3$ population can be observed. The emission from NO rises promptly after the laser pulse, and slowly reaches its peak at $t = 470$ and 150 $\mu$s for the $v = 1$ and 2 states, respectively. The fast and slow

vibrational excitations suggest that vibrational energy transfer (VET) to NO proceeds by more than one mechanism, as discussed in Section IV. The population of the spin−orbit ground state of NO, $^2\Pi_{1/2}$, is slightly preferred with a ratio of 0.65:1 for $^2\Pi_{3/2}/^2\Pi_{1/2}$. This ratio, corresponding to a spin−orbit temperature of ∼400 K, remains essentially constant with time, implying a population equilibrated between the two spin−orbit states.

A small amount of CO emission, centered at 2143 $cm^{-1}$, is observed when VB is used as the precursor of $C_2H_3$ (Figure 2) and is absent with VI (Figure 3b). To estimate the amount of CO produced in the VB case, we fit the CO and HCN emission bands at $t = 200$ $\mu$s, when the emissions of CO and HCN can be clearly distinguished. The intensities are then corrected for the rotationless Einstein *A* coefficients derived from corresponding absorption band intensities for CO and the $\nu_3$ band of HCN. The populations from the fit are extrapolated to include $v = 0$ of CO and $v_3 = 0$ of HCN populations assuming vibrational Boltzmann distributions for CO and all the modes of HCN. The net removal speeds of CO and HCN from the observation volume are also assumed to be identical. The derived branching ratio of CO/HCN is $0.20 \pm 0.05$, where the error bar is derived from the $1\sigma$ uncertainty in the Boltzmann population fits for each species.

In contrast, when MVK is used as the vinyl precursor (Figure 3a), the strong CO emission rises abruptly following photolysis, monotonically decays thereafter, and is observed with or without NO. Therefore, the vast majority of this CO arises from photodissociation of MVK.[19] To determine whether any of the CO observed with MVK could arise from chemical reactions, we collected emission through a band-pass filter centered on the CO emission region to increase the signal-to-noise (S/N) ratio. To within experimental error (with S/N = 30), data taken with and without NO do not show significant difference, indicating that <4% of the CO observed could be produced from chemical reaction. Experiments are also performed with either He or Ar buffer at different total pressures. The relative CO signal intensity, compared with HBr or HCN, shows little variation, indicating that relaxation of initially hot reactants has little effect on the formation of CO.

In their study of the $C_2H_3$ + NO reaction, Feng et al. assigned spectral features from low resolution TR-FTS to NCO and OH.[12] We attempted to observe emission from these two radicals in our higher resolution data. To increase the S/N ratio, we used band-pass filters centered on each region of interest to increase signal averaging times. We never observed any emission from the products of channels 1d−f.

**B. Vibrational Energy Distribution of the Products.** We are unable to obtain the spectrum of nascent HCN, because it overlaps with $C_2H_2/C_2H_3$ emission. Unfortunately, higher vibrational states of HCN have significant relaxation rate coefficients, and spectra at long time delay cannot correctly reflect the nascent vibrational distribution of HCN. Fortunately, the emission from $CH_2O$ (the coproduct of HCN) suffers little from spectral overlap with other species, and we can extract its vibrational temperature as a function of time, as shown in Figure 6 with VI as the precursor. To extract the nascent vibrational temperature of $CH_2O$, we extrapolate the temperature profile in Figure 6 to $t = 0$ using either an exponential or linear functional form. Under our conditions, production and relaxation of $CH_2O$ occur on similar time scales. An accurate relaxation model of $CH_2O$ requires detailed knowledge of the relaxation rates of different vibrational states, which is beyond the scope of the current study. Given this complexity, it is not clear what

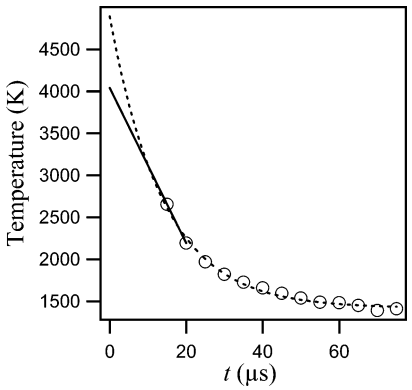


**Figure 6.** Vibrational temperature of $CH_2O$ at different time delays. The linear and exponential extrapolations to $t = 0$ are shown as the solid and dotted lines, respectively.

functional form the temperature profile should follow. Instead, we use a linear extrapolation using only the first two data points, or an exponential extrapolation using all the data points. Considering the shape of the profile in Figure 6, these limits should bound the true nascent temperature. The linear extrapolation gives a temperature of 4000 K, corresponding to $\langle E_{vib} \rangle \sim$ 36 kcal/mol, whereas the exponential extrapolation gives 4900 K, or $\langle E_{vib} \rangle \sim$ 47 kcal/mol, assuming all modes of $CH_2O$ are equilibrated at these temperatures.

**C. Electronic Structure and Rate Coefficient Calculations.** To aid in interpreting the source of CO observed by Sherwood and Gunning and in the current experiment with VB as the precursor, we performed theoretical calculations to complete the PES of channel 1c, which produces CO. For the pathway Sumathi et al.[10] found to CO + $H_2CNH$, the highest barrier is either 38.4 or 44.2 kcal/mol above reactants with MP2 or CCSD(T) theory, respectively. Striebel et al.[11] recently found a lower energy pathway to CO through a bicyclic intermediate, with a barrier height only ∼0.9 kcal/mol above the reactants, shown as the solid line in Figure 1. However, they did not calculate the PES beyond the $CH_2NCHO$ well, or the thermal rate coefficient for this channel.

Referring to Figure 1, we calculated the geometric structures and vibrational frequencies of TS5 ($CH_2NCHO \rightarrow H_2CNH$ + CO), $H_2CNH$, and CO via density functional theory employing the Becke-3 Lee−Yang−Parr (B3LYP) functional and the 6-311++G(d,p) basis set. The energies are calculated employing the QCISD(T) method with Dunning's cc-pVTZ and cc-pVQZ basis sets and are extrapolated to the infinite basis set limit. The 0 K heats of formation are evaluated by referencing theoretical to experimental heats of formation for $H_2$, $CH_4$, $CO_2$, and $N_2$. Zero-point energy corrections at the B3LYP/6-311++G(d,p) level of theory are incorporated in all the energies. We find the heat of formation of TS5 to be 69.1 kcal/mol, which is 25.2 kcal/mol below the reactant asymptote and 26.1 kcal/mol below the highest, rate-limiting barrier (TS3) on the channel 1c PES. We calculated the microcanonical rate coefficients by RRKM theory (using the saddlepoint properties predicted by the ab initio calculations) with the Variflex program.[36] The microcanonical rate coefficients for the rate-limiting steps toward channels 1b and 1c are shown in Figure 7 for a total angular momentum $J = 2$. The rate coefficients with different angular momenta are expected to have only minor differences. The branching ratio of channel 1c is predicted to be 0.018% by calculating the zero pressure thermal rate coefficients at 300 K. This branching ratio increases to 0.065% and 0.19% by decreasing the energy of the rate-limiting barrier (TS3) by 1 and 2 kcal/mol, respectively. Both of the energy changes are

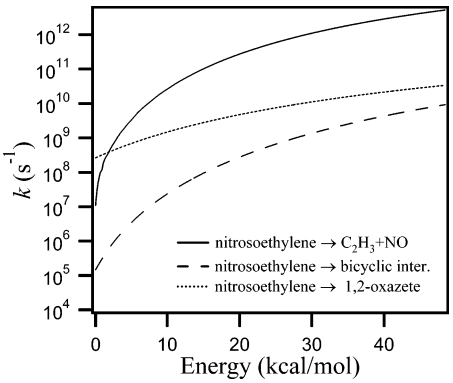


**Figure 7.** Microcanonical rate coefficients for decomposition of nitrosoethylene to reactants (channel 1a), 1,2-oxazete (leading to channel 1b), and the bicyclic intermediate (leading to channel 1c).

within reasonable error bounds of the quantum chemical prediction. The branching ratio changes only very little with pressure up to 10 Torr and then drops rapidly with increasing pressure beyond that point.

**D. Possible Secondary Reactions and Their Effects on the Observed Emission Spectra.** Since the reaction is laser-initiated and several kinds of atoms and radicals are produced upon UV photolysis, it is necessary to evaluate the importance of possible secondary chemistry in the system. The 193 nm photodissociation of vinyl bromide proceeds via multiple channels: $C_2H_3$ + Br ($^2P_J$) (56%) and $C_2H_2$ (acetylene, vinylidene) + HBr (44%).[34] It is generally believed that upon the absorption of a 193 nm photon, the C−Br bond breaking occurs on repulsive electronically excited potential energy surfaces, whereas the HBr elimination channels proceed on the ground surface through fast internal conversion of optically prepared excited vinyl bromide.[37−40] Both experimental[39,40] and theoretical[38,41] studies indicate that HBr arises primarily from the three-center elimination, which, at least transiently, forms $H_2CC$ (vinylidene) + HBr. The Lennard-Jones collision frequency between $C_2H_2$ and helium is ∼12.4 $\mu s^{-1}$ $Torr^{-1}$, while the lifetime of ground-state singlet vinylidene is estimated to be 0.04−0.2 ps.[42] Although some recent theoretical[43,44] and experimental[45] studies support a much longer lifetime of ground state singlet vinylidene with an internal energy near or below the isomerization threshold, the lifetime of any nascent singlet vinylidene from vinyl bromide photolysis is expected to be significantly reduced because it contains a large amount of internal energy, averaging 24 kcal/mol.[40] Therefore, the potentially highly reactive singlet vinylidene is expected to quickly isomerize to acetylene before colliding with surrounding molecules. Neither HBr nor acetylene react with either vinyl bromide or NO near room temperature. Fahr and Laufer reported formation of triplet vinylidene ($^3B_2$) during the VUV photolysis of acrylonitrile ($C_2H_3CN$)[46] and vinyl chloride ($C_2H_3Cl$).[47] If triplet vinylidene is formed from VB, its much longer lifetime (compared to singlet vinylidene) might introduce some important side reactions (see section IV).

As far as we know, there is no report on the reaction of vinyl bromide with bromine atoms. However, the reaction of bromine atoms with ethylene or substituted ethylene generally produces only association products at sufficiently high pressure, and should be of minor importance at the low pressures in the present experiment. Another possible three-body recombination reaction of bromine atoms is Br + NO + M, yielding BrNO as the primary product at room temperature, but the reaction rate is extremely slow under the current experimental conditions,[48] and can therefore be ignored. There are few studies of photodissociation of VI at 248 nm. Yamashita reported a yield of 81% for the $C_2H_3$ + I channel at 254 nm.[49] Our preliminary TR-FTS experiments indicate that the dissociation proceeds exclusively via simple C−I bond fission resulting in vinyl + I as the only products at 248 nm. Further experiments on the photofragment energy distribution and the dissociation branching ratio are underway. The presence of I, HI (if any), and acetylene should have negligible effect on the data analysis.

The quantum yield of methyl and vinyl radicals from the photodissociation of methyl vinyl ketone at 193 nm has been determined to be ∼1 according to Fahr et al.[19] At ambient temperature, the dominant product of the $CH_3$ + NO reaction is nitrosomethane with sufficient collisional stabilization,[50] and we expect this reaction is of little importance considering the low pressure of the present experiment.

There is no measurement of the reaction of vinyl with VB, MVK, and VI. Reactions of vinyl with ethylene and acetone indicate these reactions may be important at elevated temperatures with products quite different from channels 1b−f. Some secondary reactions, i.e., vinyl + HX (X = Br, I),[51] vinyl + acetylene,[52] and vinyl + $CH_3$,[53] may have significant rate coefficients, but they should be of minor importance given the large excess of NO.

## IV. Discussion

**A. Product Channels in the $C_2H_3$ + NO Reaction.** We have made the determination of products in the title reaction more definitive by utilizing three different vinyl precursors, which are independently known to produce vinyl radicals as their major photodissociation pathway. We observe NO, HCN, and $CH_2O$ as the only common emitters among the three precursors. Furthermore, careful investigation of the formation kinetics has established that HCN and $CH_2O$ have temporal profiles consistent with reactive production from $C_2H_3$ + NO,[11] and are only present when NO is present. Considering the simplest possible statistical distribution of energy among the 10 vibrational and 3 relative translational modes of the HCN + $CH_2O$ products, the value we extract for the average nascent vibrational energy of $CH_2O$ (36−47 kcal/mol) represents a statistically reasonable deposition of available energy in this fragment. Therefore, we conclude that HCN + $CH_2O$ is the major product channel of the title reaction. The third molecule observed in emission from all three precursors, NO, is excited through VET processes. The temporal profile and product state distribution of NO reflect details of the reaction mechanism, as discussed below. The absence of reactively produced CO in both VI and MVK experiments suggests that CO is not a product of the thermalized $C_2H_3$ + NO reaction. Our observation that [CO]/[HCN] ∼ 0.20 ± 0.05 when vinyl bromide is used as the precursor is inconsistent with our RRKM calculations, which predict at most a 0.0019 branching ratio for CO via the bicyclic intermediate pathway in Figure 1. Taken together, this evidence suggests that the CO observed when VB is the precursor arises from a competing reaction, not from $C_2H_3$ + NO.

The observation that HCN + $CH_2O$ is the dominant reaction channel agrees well with the RRKM-based master equation calculation by Striebel et al.[11] Considering stabilization of nitrosoethylene ($C_2H_3NO$) or formation of HCN + $CH_2O$ as the only two outcomes of the reaction, they calculated a branching fraction to HCN + $CH_2O$ that is close to unity at low pressure, and remains >0.9 with pressure up to ∼10 Torr at 300 K. The calculated branching to HCN + $CH_2O$ increases slightly from 0.94 to 0.96 with an increase in temperature from 300 to 700 K at 10 Torr. Under our low-pressure experimental conditions, stabilization of nitrosoethylene is a negligible process.

It is tempting to try to extract a rate coefficient from the temporal profile of $CH_2O$ in our time-resolved spectra. Unfortunately, the low total pressure and rather high NO concentration required in our experiment lead to overlapping time scales for product formation and the relaxation of hot products. These overlapping processes, combined with the fact that different vibrational levels of $CH_2O$ likely have different VET rates, lead to a complex formaldehyde profile that cannot be described by a simple model.

Channels 1d−f are much less exothermic compared with channels 1b and 1c. Therefore, the energy partitioned into vibrational modes for these three channels is expected to be less. However, the available energy is high enough to populate the first several vibrational states of the possible products. The available vibrational relaxation measurements of some of the molecules in channels 1d−f[54,55] indicate that the relaxations may have rate coefficients of 0.05−0.5 $\mu s^{-1}$ at 1 Torr. The fast relaxation indicates that the emission from these molecules may be observed only in the first few traces of the TR-FTS spectrum and might be buried in the noise background, which is more pronounced for data at short delay times. However, experiments performed with band-pass filters to increase the S/N ratio of data show no clear signals from NCO or OH, and we conclude that these channels are not produced. Feng et al. reported the existence of NCO and OH as the reaction products of $C_2H_3$ + NO using TR-FTS spectroscopy with a resolution of 16 $cm^{-1}$.[12] Since NO and NCO emissions (∼1800 $cm^{-1}$) as well as emissions of OH, HCN, HCCH, and $C_2H_3$ (>3000 $cm^{-1}$) will be rotationally unresolved or at best partially resolved at 16 $cm^{-1}$ resolution, these features may severely overlap. Such low resolution makes band assignment difficult and may lead to erroneous conclusions.

**B. Potential Energy Surface and the Reaction Mechanism.** The schematic PES of channels 1b and 1c is shown in Figure 1. Our RRKM calculations show that the isomerization of nitrosoethylene to 1,2-oxazete and to the bicyclic intermediate are the rate-limiting steps for channels 1b and 1c, respectively. The microcanonical rate coefficients in Figure 7 show that, at high energy, the dissociation of nitrosoethylene back to reactants is generally more than 2 orders of magnitude faster than the isomerization of nitrosoethylene to the ring-containing intermediates, and the dominant process at high energy is the formation−dissociation equilibrium of the nitrosoethylene adduct.

$$C_2H_3 + NO \leftrightarrow C_2H_3NO \qquad (2)$$

In a bath gas at ambient temperature, the photolytically produced, vibrationally excited vinyl radical will relax to the vibrational ground state by collisional energy transfer. The formation−dissociation equilibrium of nitrosoethylene should facilitate this relaxation. Enhancement of collisional energy transfer by the formation of long-lived collision complexes is supported by both experimental and theoretical studies,[56−58] and our spectra provide evidence for this mechanism in the $C_2H_3$ + NO reaction.

The infrared emission we observe from NO arises from collisions of NO $v = 0$ with vibrationally hot molecules. The rise of NO emission in Figure 5 cannot be characterized by a single exponential function. Instead, there is a prompt rise of vibrationally excited NO in both $v = 1$ and 2, followed by a slower rise, implying two pathways for VET. Furthermore, $\Delta v = +1$ excitations by collisional energy transfer are generally much more probable than $\Delta v = +2$ excitations. We propose that the prompt rise of NO $v = 1$ and especially $v = 2$ after the laser flash is evidence of the decomposition of nitrosoethylene back to reactants. Because NO is present in great excess, it is unlikely that prompt NO $v = 2$ production occurs via two successive $\Delta v = +1$ collisions. Instead, the covalent interaction between NO and vinyl in the nitrosoethylene adduct significantly facilitates energy transfer, allowing prompt production of NO $v = 2$. The slower rise of the $v = 1$ (and to a lesser extent $v = 2$) populations may be attributed to collisions between NO and hot molecules (reactants or products) without forming a complex. Similar NO temporal profiles are also observed in VI and MVK experiments.

The existence of fast VET is also supported by the fast decay of vinyl emission (<5 $\mu s$) when NO is present. From our data we obtain a lower limit of the rate coefficient for vinyl relaxation by NO of $3 \times 10^{-11}$ $cm^3$ $molecule^{-1}$. Howard and Smith[59] have proposed that the rate coefficient for a bimolecular association reaction in the high-pressure limit ($k_\infty$) can be estimated by measuring the rate of vibrational relaxation of one reactant by the other ($k_{relax}$). Using this correspondence, our determination of $k_\infty = k_{relax} \geq 3 \times 10^{-11}$ $cm^3$ $molecule^{-1}$ is consistent with the value of $k_\infty$ found by Striebel et al.[11] to appropriately model their pressure-dependent data.

The microcanonical rate coefficients in Figure 7 show that as $C_2H_3NO$ is either formed from reactants with less energy or loses energy due to collisions, its dissociation back to reactants is less important and its isomerization, leading ultimately to HCN + $CH_2O$, begins to compete kinetically. Therefore, the low-energy part of the population makes the major contribution to the reactive flux. The opening of the HCN + $CH_2O$ product channel as the energy decreases is a result of kinetic competition between the loose transition state for dissociation of $C_2H_3NO$ back to reactants and the tight, lower energy transition state (TS1) leading to products. At high energy, the greater entropy of the loose transition state effectively shuts off the product channels. As energy is removed from $C_2H_3NO$, the substantially lower energy of TS1 compared to reactants allows this pathway to compete with redissociation despite entropy loss in forming a four-member ring in the 1,2-oxazete intermediate. At higher pressures, collisions can remove energy sufficiently rapidly from $C_2H_3NO$ to stabilize it in the nitrosoethylene well, inhibiting both redissociation and product formation. However, in our low-pressure environment, stabilization of nitrosoethylene cannot compete with the other two processes. This mechanism, where deactivation enhances product formation, also suggests that changes of branching ratios at different temperatures may be small, since these ratios will be primarily determined by the branching ratios of the low energy portion of the population distribution. This picture is consistent with the experimental observations of Striebel et al.,[11] in which the measured thermal rate coefficient shows little pressure dependence at 300 K and some at higher temperatures. Only a relatively small variation of the branching ratio of channel 1b is predicted by their master equation calculation from 300 to 700 K.

The absence of CO as a reaction product when VI and MVK are used strongly indicates that the CO we observe must arise from reactions other than $C_2H_3$ + NO. The upper bound of the calculated branching ratio of channel 1c at zero pressure and 300 K, 0.19%, is still far less than the observed ratio [CO]/[HCN] = (20 ± 5)% when VB is used. However, it is necessary to consider the theoretical branching ratio at higher temperature because the nascent vinyl radical is highly vibrationally excited. Figure 7 suggests that channel 1c might play a minor role at higher energies, because the microcanonical rate of channel 1c increases faster than the rate of channel 1b with increasing

energy. The average total translational energy of $C_2H_3$ + Br from 193 nm photodissociation of vinyl bromide is measured to be 42 ± 3 kcal/mol,[34] implying an average internal energy of vinyl radicals of 29 ± 3 kcal/mol, assuming ground-state Br and a C−Br bond strength of 77 kcal/mol. The ratio of our calculated microcanonical rate coefficients for the formation of 1,2-oxazete and the bicyclic intermediate (rate-limiting steps for channels 1b and 1c, respectively) is 9:1 at 29 kcal/mol, giving a calculated branching ratio of channel 1c at this energy of 10%. However, less than 1% of $C_2H_3$ + NO collisions at such high energies can form products due to the much more efficient redissociation of nitrosoethylene back to reactants at these energies. The redissociation process effectively cools the $C_2H_3$ reactant, thus yielding little change from the thermal branching ratio. Therefore, very little CO is expected even from hot $C_2H_3$, a prediction that is in agreement with our experimental data.

**C. Other Sources of CO Production.** If the title reaction formed NCO via channel 1d, the secondary reaction of NCO + NO would produce CO. The two channels for the reaction of NCO with NO,

$$\mathrm{NCO + NO \rightarrow N_2O + CO} \qquad \Delta_r H^\circ_{298K} = -66.4 \text{ kcal/mol} \tag{3a}$$

$$\mathrm{NCO + NO \rightarrow N_2 + CO_2} \qquad \Delta_r H^\circ_{298K} = -153.7 \text{ kcal/mol} \tag{3b}$$

have comparable branching ratios at room temperature. Two measurements of the branching ratios of channels 3a/3b, 0.44:0.56[60] and 0.35:0.65,[61] are in reasonable agreement with each other. However, we do not observe any emission from NCO at 1921 $cm^{-1}$, which should be rotationally resolved at the current resolution.[62] Furthermore, $CO_2$ and $N_2O$ are exceptionally strong emitters in the infrared, and the absence of these emissions argues strongly against the presence of NCO.

The reaction of acetylene with NO is predicted to produce HCO + HCN as the dominant products at low pressure and high temperature.[63] HCO with sufficient internal energy may dissociate to H + CO. However, even for acetylene with an average internal energy of 24 kcal/mol (~3200 K), the rate coefficient of $C_2H_2$ + NO is still ~20 times smaller than the vinyl + NO reaction and cannot account for the CO observed.[63] The small variation of relative CO signal intensity at different total pressures with different buffer gases also suggests that the $C_2H_2$ + NO reaction is negligible.

Given the 88 kcal/mol exothermicity of channel 1b, another possible source of CO is the unimolecular decomposition of $CH_2O$ via $CH_2O \rightarrow H_2 + CO$. This dissociation of formaldehyde is nearly thermoneutral, but kinetically inhibited by a barrier of 79.2 ± 0.8 kcal/mol with respect to $CH_2O$.[64] For $E \geq 80$ kcal/mol, the unimolecular dissociation rate coefficient $k_{uni} \geq 10^8\ s^{-1}$.[64] This energy threshold represents 91% of the available energy in channel 1b, an unlikely, though not impossible outcome of the title reaction. In addition, formaldehyde is also formed when MVK and VI are the vinyl precursors, but reactively produced CO is not observed in these cases. Therefore it seems unlikely that formaldehyde decomposition is the source of CO in the VB experiments.

A final possibility for the reactive production of CO is the reaction of triplet vinylidene ($^3B_2$) with NO. As mentioned earlier, Fahr and Laufer observed the formation of triplet vinylidene during the vacuum-ultraviolet photolysis (120−180 nm) of $C_2H_3CN$[46] and $C_2H_3Cl$[47] by monitoring the VUV absorption of triplet vinylidene at 137 nm. The active photolysis wavelength may be in the longer wavelength region according to the absorption spectra of acrylonitrile and vinyl chloride.[46] The UV absorption spectra of similar halogenated aliphatic hydrocarbons are generally red-shifted when Cl is substituted by Br. Therefore, the photolysis at 193 nm of vinyl bromide might produce triplet vinylidene. If the source of the CO is the $H_2C{=}C$ ($^3B_2$) + NO reaction, the absence of reactively produced CO in MVK and VI experiments can be readily explained. The quantum yield of vinyl from MVK photolysis at 193 nm is close to unity, indicating negligible presence of the $C_2H_2$ species. For VI, the 248 nm photon energy is not sufficiently energetic to produce triplet vinylidene. Further research on triplet vinylidene reactions will be required to test this hypothesis of CO formation. CO is also a minor product in Sherwood and Gunning's experiments. In their experiments,[65] the ratio of CO produced with respect to HCN ranges from 4% to 13% and might be a product from the secondary reaction of Hg photosensitized dissociation of formaldehyde.

## V. Conclusion

We have studied the $C_2H_3$ + NO reaction using TR-FTS spectroscopy. The emission spectra indicate that HCN + $CH_2O$ is the dominant channel near 300 K, in agreement with the predictions of RRKM-based master equation calculations from ref 11 and from this work. In contrast to Feng et al.'s assignment of OH and NCO products,[12] we did not observe any emission from the products of channels 1c−e, suggesting that these channels are negligible at room temperature. We do observe CO emission with VB as the vinyl radical precursor. However, the absence of CO as a reaction product when MVK and VI are used strongly indicates that it arises from a secondary reaction. Our observation of only bimolecular products disagrees with Sumathi et al.'s[10] conclusion that near 300 K the reaction cannot proceed beyond formation of 1,2-oxazete. The reaction mechanism proposed by Striebel et al.,[11] and confirmed here, suggests that the temperature dependence of the product branching ratio is less sensitive to temperature than one might expect because the low energy portion of the Boltzmann distribution contributes disproportionately to the reactive flux.

**Acknowledgment.** The authors thank Dr. Craig Taatjes for helpful discussions, Gary Wilke and Howard Johnsen for their technical support, and the reviewers for helpful comments. This research is supported by the Division of Chemical Sciences, Geosciences, and Biosciences, the Office of Basic Energy Sciences of the U.S. Department of Energy. Sandia is a multiprogram laboratory operated by Sandia Corporation, a Lockheed Martin Company, for the United States Department of Energy's National Nuclear Security Administration under contract DE-AC04-94AL85000.

## References and Notes

(1) See for example: Simmie, J. M. *Prog. Energy Combust. Sci.* **2003**, *29*, 599. Miller, J. A.; Kee, R. J.; Westbrook, C. K. *Annu. Rev. Phys. Chem.* **1990**, *41*, 345; and references therein.

(2) Richter, H.; Howard, J. B. *Prog. Energy Combust. Sci.* **2000**, *26*, 565.

(3) Wendt, J. O. L.; Sternling, C. V.; Matovich, M. A. *Proc. Combust. Inst.* **1973**, *14*, 897.

(4) Prada, L.; Miller, J. A. *Combust. Sci. Technol.* **1998**, *132*, 225.

(5) Sherwood, A. G.; Gunning, H. E. *J. Am. Chem. Soc.* **1963**, *85*, 3506.

(6) Sherwood, A. G.; Gunning, H. E. *J. Phys. Chem.* **1965**, *69*, 1732.

(7) Benson, S. W. *Int. J. Chem. Kinet.* **1994**, *26*, 997.

(8) Ogura, H. *Bull. Chem. Soc. Jpn.* **1978**, *51*, 3418.

(9) Arulmozhiraja, S.; Kolandaivel, P. *THEOCHEM* **1998**, *429*, 165.

(10) Sumathi, R.; Nguyen, H. M. T.; Nguyen, M. T.; Peeters, J. *J. Phys. Chem. A* **2000**, *104*, 1905.

(11) Striebel, F.; Jusinski, L. E.; Fahr, A.; Halpern, J. B.; Klippenstein, S. J.; Taatjes, C. A. *Phys. Chem. Chem. Phys.* **2004**, *6*, 2216.

(12) Feng, W.; Wang, B.; Wang, H.; Kong, F. *Acta Physicochimica Sinica.* **2000**, *16*, 776.
(13) The heat of formation of $H_2C{=}NH$ has been measured by three groups as listed on the NIST Chemistry Webbook. Two measurements are ~26 kcal/mol, while the third is ~16 kcal/mol. We use 26 kcal/mol in the paper, because this value is closer to the result of our high level theoretical calculations.
(14) Osborn, D. L. *J. Phys. Chem. A* **2003**, *107*, 3728.
(15) Clegg, S. M.; Parsons, B. F.; Klippenstein, S. J.; Osborn, D. L. *J. Chem. Phys.* **2003**, *119*, 7222.
(16) Welsh, H. L.; Cumming, C.; Stanbury, E. J. *J. Opt. Soc. Am.* **1955**, *45*, 338.
(17) Seakins, P. W. *The Chemical Dynamics and Kinetics of Small Radicals*; Liu, K., Wagner A., Eds.; World Scientific: Singapore, 1995; p 250.
(18) Orkin, V. L.; Louis, F.; Huie, R. E.; Kurylo, M. J. *J. Phys. Chem. A* **2002**, *106*, 10195.
(19) Fahr, A.; Braun, W.; Laufer, A. H. *J. Phys. Chem.* **1993**, *97*, 1502.
(20) Blank, D. A.; Sun, W.; Suits, A. G.; Lee, Y. T.; North, S. W.; Hall, G. E. *J. Chem. Phys.* **1998**, *108*, 5414.
(21) Robinson, J. C.; Harris, S. A.; Sun, W. Z.; Sveum, N. E.; Neumark, D. M. *J. Am. Chem. Soc.* **2002**, *124*, 10211.
(22) Zou, P.; Osborn, D. L. *Phys. Chem. Chem. Phys.* **2004**, *6*, 1697.
(23) Chen, D. W.; Rao, K. N.; McDowell, R. S. *J. Mol. Spectrosc.* **1976**, *61*, 71.
(24) Nishimiya, N.; Yukiya, T.; Ohtsuka, T.; Suzuki, M. *J. Mol. Spectrosc.* **1997**, *182*, 309.
(25) Amiot, C.; Verges, J. *J. Mol. Spectrosc.* **1980**, *81*, 424.
(26) Lyulin, O. M.; Perevalov, V. I.; Tashkun S. A.; Teffo, J.-L. *Proc. SPIE* **2000**, *4063*, 126.
(27) Smith, A. M.; Coy, S. L.; Klemperer, W.; Lehmann, K. K. *J. Mol. Spectrosc.* **1989**, *134*, 134.
(28) Clouthier, D. J.; Ramsay, D. A. *Annu. Rev. Phys. Chem.* **1983**, *34*, 31.
(29) Bouwens, R. J.; Hammerschmidt, J. A.; Grzeskowiak, M. M.; Stegink, T. A.; Yorba, P. M.; Polik, W. F. *J. Chem. Phys.* **1996**, *104*, 460.
(30) Kelly, R. L. *J. Phys. Chem. Ref. Data* **1987**, *16*, Suppl. 1.
(31) Watson, J. K. G. *Vibrational Spectra and Structure*; Durig, J. R., Ed.; Elsevier North-Holland: New York, 1977; Vol. 6, pp 1−90.
(32) Nakanaga, T.; Kondo, S.; Saëki, S. *J. Chem. Phys.* **1982**, *76*, 3860.
(33) Letendre, L.; Liu, D.-K.; Pibel, C. D.; Halpern, J. B.; Dai, H.-L. *J. Chem. Phys.* **2000**, *112*, 9209. Sattelmeyer, K. W.; Schaefer, H. F., III *J. Chem. Phys.* **2002**, *117*, 7914.
(34) Wodtke, A. M.; Hintsa, E. J.; Somorjai, J.; Lee, Y. T. *Isr. J. Chem.* **1989**, *29*, 383.
(35) Frost, M. J.; Smith, I. W. M. *Chem. Phys. Lett.* **1992**, *191*, 574. Frost, M. J.; Smith, I. W. M. *J. Chem. Phys.* **1995**, *99*, 1094.
(36) Klippenstein, S. J.; Wagner, A. F.; Dunbar, R. C.; Wardlaw, D. M.; Robertson, S. H.; Miller, J. A. VARIFLEX version 1.12m, 2002.
(37) Blank, D. A.; Sun, W.; Suits, A. G.; Lee, Y. T. *J. Chem. Phys.* **1998**, *108*, 5414.
(38) Mains, G. J.; Raff, L. M.; Abrash, S. A. *J. Phys. Chem.* **1995**, *99*, 3532.
(39) Lin, S.-R.; Lin, S.-C.; Lee, Y.-C.; Chou, Y.-C.; Chen, I.-C.; Lee, Y.-P. *J. Chem. Phys.* **2001**, *114*, 7396.
(40) Liu, D.-K.; Letendre, L. T.; Dai, H.-L. *J. Chem. Phys.* **2001**, *115*, 1734.
(41) Kay, R. D.; Raff, L. M. *J. Phys. Chem. A* **1997**, *101*, 1007.
(42) Ervin, K. M.; Ho, J.; Lineberger, W. C. *J. Chem. Phys.* **1989**, *91*, 5974.
(43) Schork, R.; Köppel, H. *J. Chem. Phys.* **2001**, *115*, 7907.
(44) Hayes, R. L.; Fattal, E.; Govind, N.; Carter, E. A. *J. Am. Chem. Soc.* **2001**, *123*, 641.
(45) Levin, J.; Feldman, H.; Baer, A.; Ben-Hamu, D.; Heber, O.; Zajfman, D.; Vager, Z. *Phys. Rev. Lett.* **1998**, *81*, 3347.
(46) Fahr, A.; Laufer, A. H. *J. Phys. Chem.* **1992**, *96*, 4217.
(47) Fahr, A.; Laufer, A. H. *J. Phys. Chem.* **1985**, *89*, 2906.
(48) Dolson, D. A.; Klingshirn, M. D. *J. Phys. Chem.* **1993**, *97*, 6645.
(49) Yamashita, S. *Chem. Lett.* **1975**, *9*, 967.
(50) Kaiser, E. W. *J. Phys. Chem.* **1993**, *97*, 11681.
(51) Seetula, J. A. In *Annales Academiae Scientiarum Fennicae*; Series A, II. Chemica; Suomalainen Tiedeakatemia: Helsinki, 1991; pp 1−45.
(52) Knyazev, V. D.; Stoliarov, S. I.; Slagle, I. R. *Proc. Combust. Inst.* **1996**, *26*, 513.
(53) Fahr, A.; Laufer, A. H.; Tardy, D. C. *J. Phys. Chem. A* **1999**, *103*, 8433.
(54) Hancock, G.; McKendrick, K. G. *Chem. Phys. Lett.* **1986**, *127*, 125.
(55) Smith, I. W. M.; Williams, M. D. *J. Chem. Soc., Faraday Trans. 2* (*UK*) **1985**, *81*, 1849.
(56) Langford, A. O.; Moore, C. B. *J. Chem. Phys.* **1984**, *80*, 4211.
(57) Glänzer, K.; Troe, J. *J. Chem. Phys.* **1976**, *65*, 4324.
(58) Bhattacharjee, R. C.; Forst, W. *Chem. Phys.* **1978**, *30*, 217.
(59) Howard, M. J.; Smith, I. W. M. *Prog. React. Kinet.* **1983**, *12*, 55. Smith, I. W. M. *J. Chem. Soc., Faraday Trans.* **1991**, *87*, 2271.
(60) Cooper, W. F.; Park, J.; Hershberger, J. F. *J. Phys. Chem.* **1993**, *97*, 3283.
(61) Becker, K. H.; Kurtenbach, R.; Wiesen, P. *Chem. Phys. Lett.* **1992**, *198*, 424.
(62) Barnes, C. E.; Brown, J. M.; Fackerell, A. D.; Sears, T. J. *J. Mol. Spectrosc.* **1982**, *92*, 485.
(63) Nguyen, H. M. T.; Sumathi, R.; Nguyen, M. T. *J. Phys. Chem.* **1999**, *103*, 5015.
(64) Polik, W. F.; Guyer, D. R.; Moore, C. B. *J. Chem. Phys.* **1990**, *92*, 3453.
(65) Harrison, A. G.; Lossing, F. P. *Can. J. Chem.* **1960**, *38*, 544.